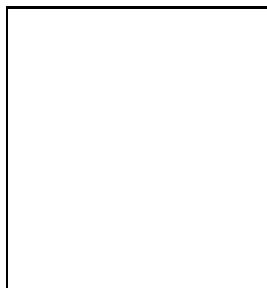


## BARYONIC $B$ DECAYS

J. SCHÜMANN, for the Belle Collaboration

*Department of Physics, High Energy Physics Group, National Taiwan University  
No.1, Sec.4 Roosevelt Rd., 106 Taipei, Taiwan*



We summarize recent results of baryonic  $B$  decays from Belle and BaBar. The results from Belle are based on  $140 \text{ fb}^{-1}$  and results from BaBar are based on  $81 \text{ fb}^{-1}$  of data collected at the  $\Upsilon(4S)$  resonance at KEKB or PEP-II respectively. We report the results of two- and three-body baryonic  $B$  decays as well as searches for pentaquarks. The three-body baryonic  $B$  decays display an enhancement in the low mass region, which is not in agreement with general phase space expectations.

### 1 Introduction

Baryonic  $B$  decays are a unique feature of  $B$  meson decays and have already been well established through previous measurements<sup>1,2,3,4</sup>. Three-body baryonic  $B$  decays were found to have a larger branching fraction than two-body decays.

Three-body baryonic  $B$  decays display the common feature of a peaking behaviour toward the baryon-antibaryon pair mass threshold. This feature has also been observed in baryonic  $J/\Psi$  decays<sup>5</sup>, indicating it may be a universal feature of these decays. Possible explanations include intermediate (gluonic) resonant states or non-perturbative QCD effects of the quark fragmentation process<sup>6,7,8,9</sup>. Angular distributions are used to discriminate between the different decay mechanisms.

### 2 The analyses

#### 2.1 Event Selection

We use a data sample of  $152 \times 10^6 B\bar{B}$  pairs, corresponding to an integrated luminosity of  $140 \text{ fb}^{-1}$ , collected by the Belle detector at the KEKB<sup>10</sup> asymmetric energy  $e^+e^-$  collider. The detector is described in detail elsewhere<sup>11</sup>.

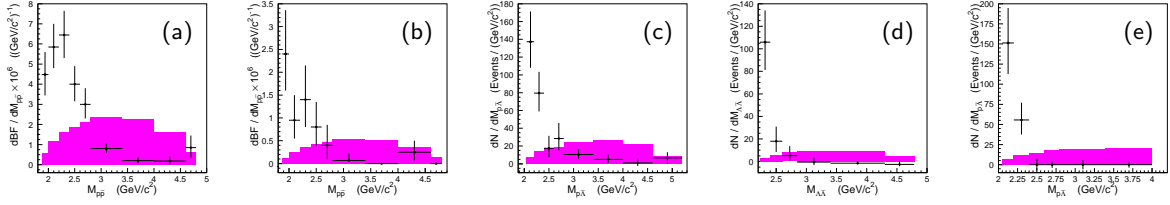


Figure 1: Differential branching fractions for (a)  $B^+ \rightarrow p\bar{p}K^+$ , (b)  $B^+ \rightarrow p\bar{p}K_S$ , (c)  $B^0 \rightarrow p\bar{\Lambda}\pi^-$ , (d)  $B^+ \rightarrow \Lambda\bar{\Lambda}K^+$  and (e)  $B^+ \rightarrow p\bar{\Lambda}\gamma$  as a function of the baryon pair mass. The shaded distribution shows the expectation from phase-space simulations.

We select events through the following decay channels:  $\Lambda_c^+ \rightarrow pK^-\pi^+$ ,  $p\bar{K}^0$ ,  $\Lambda\pi^+$ ,  $p\bar{K}^-\pi^+\pi^-$  and  $\Lambda\pi^+\pi^-\pi^+$ ;  $\Lambda \rightarrow p\pi^-$  and  $K_S^0 \rightarrow \pi^+\pi^-$ <sup>a</sup>.

All primary charged tracks are required to satisfy track quality criteria based on the track impact parameters relative to the interaction point (IP). To identify charged tracks, the proton ( $L_p$ ), kaon ( $L_K$ ) and pion ( $L_\pi$ ) likelihoods are determined from information obtained by the hadron identification system. A track is identified as a proton if  $L_p/(L_p + L_\pi) > 0.6$  and  $L_p/(L_p + L_K) > 0.6$  (0.01), or as a kaon if  $L_K/(L_K + L_\pi) > 0.6$  (0.2), or as a pion if  $L_\pi/(L_K + L_\pi) > 0.6$  (0.05).

We require the mass of the  $\Lambda$  candidates to be consistent with the nominal  $\Lambda$  baryon mass,  $1.111$  ( $1.113$ )  $\text{GeV} < M_{p\pi^-} < 1.121$  ( $1.118$ )  $\text{GeV}$ . The values inside (without) brackets apply to the  $B \rightarrow \Lambda_c^+ \bar{p}\pi^-$  (all other) analyses.

Continuum background, the major background contribution for all decays, is suppressed in the  $B^- \rightarrow \Lambda_c^+ \bar{p}\pi^-$  decay by imposing requirements on the angle between the thrust axis of the  $B$  candidate tracks and that of other tracks, as well as on the ratio of the second to the zeroth Fox-Wolfram moment<sup>12</sup>. For all other decays, we form a Fisher discriminant<sup>13</sup> that combines seven event shape variables. Probability density functions (PDF) for the Fisher discriminant and the cosine of the angle between the  $B$  flight direction and the beam direction in the  $\Upsilon(4S)$  rest frame are combined to form the signal (background) likelihood  $\mathcal{L}_s$  ( $\mathcal{L}_b$ ). We then optimize the selection of the likelihood ratio  $\mathcal{R} = \mathcal{L}_f/(\mathcal{L}_f + \mathcal{L}_b)$  for each mode. For more details of the selection and background suppression refer to<sup>14,15,4,16,17</sup>.

## 2.2 Charmless $B$ decays

We perform an unbinned likelihood fit that maximizes the likelihood function,

$$L = \frac{e^{-(N_s+N_b)}}{N!} \prod_{i=1}^N \left[ N_s P_s(M_{bc_i}, \Delta E_i) + N_b P_b(M_{bc_i}, \Delta E_i) \right],$$

to estimate the signal yield in  $5.20 \text{ GeV}/c^2 < M_{bc} < 5.29 \text{ GeV}/c^2$  and  $-0.1 \text{ GeV} < \Delta E < 0.2 \text{ GeV}$  for  $B \rightarrow p\bar{p}K$  and  $B^0 \rightarrow p\bar{\Lambda}\pi^-$ ,  $-0.15 \text{ GeV} < \Delta E < 0.3$  for  $B^+ \rightarrow \Lambda\bar{\Lambda}K^+$  and  $-0.2 \text{ GeV} < \Delta E < 0.5$  for  $B^+ \rightarrow p\bar{\Lambda}\gamma$ ; here  $P_s$  ( $P_b$ ) denotes the signal (background) PDF,  $N$  is the number of events in the fit, and  $N_s$  and  $N_b$  are fit parameters representing the number of signal and background events, respectively.

The differential branching fractions as a function of the baryon pair mass are shown in Figure 1 after applying a charmonium veto for the  $B \rightarrow p\bar{p}K$  modes. A clear enhancement at threshold in disagreement with phase space expectations can be seen. The width of the peaking behaviour depends on the signal mode. The  $\Delta E$  distributions (with  $M_{bc} > 5.27 \text{ GeV}$ ) for the

<sup>a</sup>Charge conjugate modes are implicitly included throughout this paper

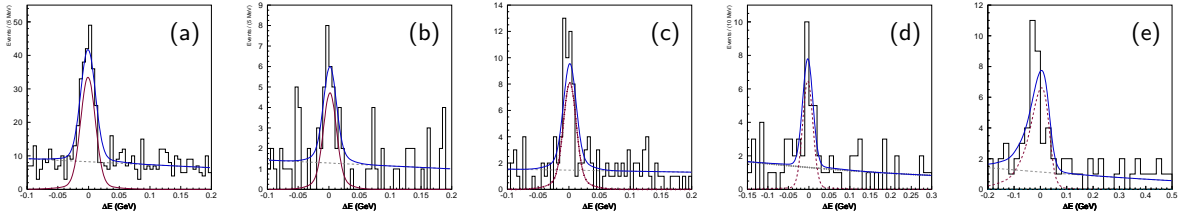


Figure 2: Distributions of the projections in  $\Delta E$  for (a)  $B^+ \rightarrow p\bar{p}K^+$ , (b)  $B^+ \rightarrow p\bar{p}K_S$ , (c)  $B^0 \rightarrow p\bar{\Lambda}\pi^-$ , (d)  $B^+ \rightarrow \Lambda\bar{\Lambda}K^+$  and (e)  $B^+ \rightarrow p\bar{\Lambda}\gamma$  with baryon-antibaryon mass less than  $2.85 \text{ GeV}/c^2$ . The solid, dotted and dashed lines represent the combined fit results, fitted signal and fitted background, respectively.

five three-body baryonic  $B$  decays are shown in Figure 2. The projections of the fit results are displayed as solid curves. The results are summarized in Table 1.

We study the angular distribution of the baryon-antibaryon system in its helicity frame. The angle  $\theta_p$  is defined as the angle between the proton direction and the meson direction in the baryon-antibaryon pair rest frame. We find an asymmetry in the angular distributions, which indicates that the fragmentation picture is favored. Antiprotons are emitted along the  $K^+$  direction most of the time, which can be explained by a parent  $\bar{b} \rightarrow \bar{s}$  penguin transition followed by  $\bar{s}u$  fragmentation into the final state. The energetic  $\bar{s}$  quark picks up the  $u$  quark from a  $u\bar{u}$  pair in vacuum and the remaining  $\bar{u}$  quark then drags a  $\bar{u}\bar{d}$  diquark out of vacuum.

Two-body charmless baryonic  $B$  decays were investigated, but no signal events were seen. For a detailed description of this analysis please read <sup>15</sup>. The upper limits are given in Table 1.

The newly observed narrow pentaquark state,  $\Theta^+$  <sup>18</sup>, can decay into  $pK_S^0$ . We perform a search in  $B^0 \rightarrow p\bar{p}K_S$  by requiring  $1.53 \text{ GeV}/c^2 < M_{pK_S^0} < 1.55 \text{ GeV}/c^2$ . We find no evidence for a pentaquark signal. We also perform a search for  $\Theta^{++}$ , which can decay to  $pK^+$  in the mode  $B^+ \rightarrow p\bar{p}K^+$  <sup>19</sup>. We find no evidence for signal. We set an upper limit assuming this state is narrow and centered near  $1.71 \text{ GeV}/c^2$ . The upper limits are listed in Table 1.

Systematic errors are studied; for a detailed description of the procedure please refer to <sup>14,15,16,4</sup>. The final systematic errors are listed in Table 1

### 2.3 $B^- \rightarrow \Lambda_c^+ \bar{p} \pi^-$

We perform a Dalitz plots analysis to investigate of the three-body charmed  $B^- \rightarrow \Lambda_c^+ \bar{p} \pi^-$  decay. The distributions for  $\Delta E$ , the mass of the  $\Lambda_c^+ \pi^-$  pair, the mass of the  $\Lambda_c^+ \bar{p}$  pair and its helicity distribution are displayed in Figure 3. The intermediate states of  $\Sigma_c(2455)^0$  and  $\Sigma_c(2520)^0$  can clearly be identified in Figure 3 (b). The branching fractions of these two-body intermediate states are given in Table 1. As in the previous analyses, the baryon-antibaryon pair shows a low mass enhancement. This can be parameterized with a Breit-Wigner peak and feed downs. The fit gives a mass of  $(3.35_{-0.02}^{+0.01}) \text{ GeV}/c^2$  and a full width of  $(0.07_{-0.03}^{+0.04}) \text{ GeV}/c^2$ . The fit yield is  $50 \pm 10$  events with a statistical significance of  $5.6\sigma$ . The angular distribution as seen in Figure 3 (c) cannot conclusively determine whether the enhancement arises from a resonance, fragmentation or final state interactions.

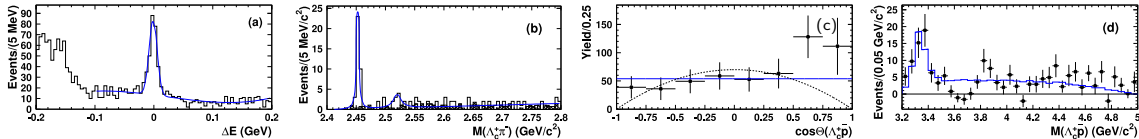


Figure 3:  $\Delta E$ ,  $\Lambda_c^+ \pi^-$  mass,  $\Lambda_c^+ \bar{p}$  helicity and its mass distribution.

Table 1: Branching fractions of the baryonic  $B$  decays. We list the decay modes, the significances, the branching fractions and the experiment that performed the analysis.

| Mode   | Significance<br>$\sigma$ | Branching fraction<br>[ $10^{-6}$ ]   | Experiment    |
|--|--------------------------|---------------------------------------|---------------|
| $\mathcal{B}(B^+ \rightarrow \Lambda \bar{\Lambda} K^+)$                                 | 7.4                      | $2.91^{+0.90}_{-0.70} \pm 0.38$       | Belle         |
| $\mathcal{B}(B^+ \rightarrow \Lambda \bar{\Lambda} \pi^+)$                               | -                        | $< 2.8$                               | Belle         |
| $\mathcal{B}(B^+ \rightarrow p \bar{p} K^+)$   | $> 10$                   | $5.30^{+0.45}_{-0.39} \pm 0.58$       | Belle         |
|  | $> 10$                   | $6.7 \pm 0.9 \pm 0.6$                 | BaBar         |
| $\mathcal{B}(B^+ \rightarrow p \bar{p} K_S)$   | $> 10$                   | $1.20^{+0.32}_{-0.22} \pm 0.14$       | Belle         |
| $\mathcal{B}(B^0 \rightarrow p \bar{\Lambda} \pi^-)$                                     | 11.2                     | $3.27^{+0.62}_{-0.51} \pm 0.39$       | Belle         |
| $\mathcal{B}(B^+ \rightarrow p \bar{\Lambda} \gamma)$                                    | 8.6                      | $2.16^{+0.58}_{-0.53} \pm 0.20$       | Belle         |
| $\mathcal{B}(p \Sigma^0 \gamma)$   | -                        | $< 4.6$                               | Belle         |
| $\mathcal{B}(B^- \rightarrow \Lambda_c^+ \bar{p} \pi^-)$                                 | 18.1                     | $201 \pm 15 \pm 20 \pm 52$            | Belle         |
| $\mathcal{B}(\Lambda_c^+ \bar{p} \text{ structure})$                                     | 6.2                      | $38.7^{+7.7}_{-7.2} \pm 4.3 \pm 10.1$ | Belle         |
| $\mathcal{B}(\Sigma_c(2455) \bar{p})$  | 8.4                      | $36.7^{+7.4}_{-6.6} \pm 3.6 \pm 9.5$  | Belle         |
| $\mathcal{B}(B \rightarrow p \bar{p} / \Lambda \bar{p} / \Lambda \bar{\Lambda})$         | -                        | $< 0.41 / 0.49 / 0.69$                | Belle         |
| $\mathcal{B}(B \rightarrow \theta^+ p) \times \mathcal{B}(\theta^+ \rightarrow K_S^0 p)$ | -                        | $< 0.23$                              | Belle         |
| $\mathcal{B}(B \rightarrow \theta^{++} p) \times \mathcal{B}(\theta^{++} K^+ p)$         | -                        | $< 0.091 / < 0.15 - 0.40$             | Belle / BaBar |

### 3 Summary

We have observed three-body charmless baryonic  $B$  decays and charmed baryonic two- and three-body decays. All three-body decays display an enhancement at threshold in the baryon-antibaryon mass. The fragmentation picture seems to be favored to explain this behaviour. The results are listed in Table 1.

### References

1. K. Abe *et al.* (Belle Collaboration), *Phys. Rev. Lett.* **88**, 181803 (2002).
2. M.Z. Wang *et al.* (Belle Collaboration), *Phys. Rev. Lett.* **90**, 201802 (2003).
3. M.Z. Wang *et al.* (Belle Collaboration), *Phys. Rev. Lett.* **92**, 131801 (2004).
4. Y.J. Lee *et al.* (Belle Collaboration), *Phys. Rev. Lett.* **93**, 211801 (2004).
5. M. Ablikim *et al.* (BES Collaboration), *Phys. Rev. Lett.* **93**, 112002 (2004).
6. W.S. Hou and A. Soni, *Phys. Rev. Lett.* **86**, 4247 (2001).
7. C.K. Chua, W.S. Hou and S.Y. Tsai, *Phys. Lett. B* **528**, 233 (2002).
8. C.K. Chua, W.S. Hou and S.Y. Tsai, *Phys. Lett. B* **544**, 139 (2002).
9. J.L. Rosner, *Phys. Rev. D* **68**, 014004 (2003).
10. S. Kurokawa and E. Kikutani, *Nucl. Instrum. Methods A* **499**, 1 (2003).
11. A. Abashian *et al.* (Belle Collaboration), *Nucl. Instrum. Methods A* **479**, 117 (2002).
12. G.C. Fox and S. Wolfram, *Phys. Rev. Lett.* **41**, 1581 (1978).
13. R.A. Fisher, *Annals of Eugenics* **7**, 179 (1936).
14. K.Abe *et.al.* (Belle Collaboration), *To be submitted to Phys. Rev. Lett.* .
15. M.-C. Chang *et.al.* (Belle Collaboration), *Phys. Rev. D* **71**, 072007 (2005).
16. M.Z. Wang *et.al.* (Belle Collaboration), Submitted to *Phys. Lett. B* (hep-ex/0503047).
17. Y.-J. Lee *et.al.* (Belle Collaboration), Submitted to *Phys. Rev. Lett.* (hep-ex/0503046).
18. See, e.g., T. Nakano *et al.* (LEPS Collaboration), *Phys. Rev. Lett.* **91**, 012002 (2003).
19. T.E. Browder, I. Klebanov and D. Marlow, *Phys. Lett. B* **587**, 62 (2004).